Heteroleptic tris-chelate ruthenium(II) complexes of N,N-disubstituted-N′-acylthioureas: Synthesis, structural studies, cytotoxic activity and confocal microscopy studies

João P. Barolli [a,*], Pedro I.S. Maia [b], Legna Colina-Vegas [a], Jane Moreira [c], Ana M. Plutin [d], Raúl Mocelo [d], Victor M. Deflon [e], Marcia R. Cominetti [f], Maria I. Camargo-Mathias [c], Alzir A. Batista [a]

[a] Departamento de Química, Universidade Federal de São Carlos, São Carlos, SP, Brazil
[b] Departamento de Química, Universidade Federal do Triângulo Mineiro, 38025-440 Uberaba, MG, Brazil
[c] Instituto de Biociências, Universidade Estadual Paulista Júlio de Mesquita Filho, Campus Rio Claro, SP, Brazil
[d] Laboratório de Síntesis Orgánica, Facultad de Química, Universidad de La Habana, La Habana, Cuba
[e] Instituto de Química de São Carlos, Universidade de São Paulo, São Carlos, SP, Brazil
[f] Departamento de Gerontologia, Universidade Federal de São Carlos, São Carlos, SP, Brazil

ABSTRACT

Ruthenium complexes have been assessed as anti-tumor agents against cancer cells. In this project, new heteroleptic ruthenium(II) complexes with general formulae [Ru(L)(bipy)(dppb)](PF$_6$) (where L = N,N-disubstituted-N′-acylthiourea, bipy = 2,2′-bipyridine and dppb = 1,4-bis(diphenylphosphino)butane) were synthesized and characterized by elemental analysis, IR and NMR (^{1}H and ^{31}P{^{1}H}) spectroscopies, molar conductivity measurements and single crystal X-ray diffractometry. The IR and NMR data suggest the coordination of the ligands to the Ru(II) metal center through the thiocarbonyl and carbonyl groups. The structures of the new complexes were further studied by X-ray crystallography, which confirmed the coordination of the ligands with the metal through the sulfur and oxygen atoms, leading to the formation of distorted octahedral complexes. The N,N-disubstituted-N′-acylthioureas and their complexes were screened with respect to their in vitro cytotoxicity. All compounds exhibited considerable antiproliferative activity against MCF-7 (human breast tumor cells ATCC HTB-26), DU-145 (human prostate tumor cells ATCC HTB-26), and relatively low toxicity against fibroblast L929 cells (health cell line from mouse ATCC CCL-1). A preliminary study regarding the mechanism of action of these compounds by confocal microscopy shows alterations of the actin filaments leading to modifications in cytoskeletal supporting the cell death and that the cell nucleus is not main target of these complexes.

© 2017 Elsevier Ltd. All rights reserved.

1. Introduction

Even after a half century of research on the theme, cancer continues to be a disease of very difficult to treatment. The main reasons for that are the diversity and complexity of tumors, drug resistance, limited animal studies and, particularly, side-effects during treatment [1]. This disease is a result of alterations in cell division involving cytoskeletal elements which leads to the disordered proliferation of tumor cells [2].

Several drug-design strategies have been employed in order to develop new drugs. Nevertheless, metal-based pharmaceuticals have generated gradual increasing interest since the serendipitous discovery of the anticancer activity of the coordination compound cis-[PtCl$_2$(NH$_3$)$_2$] (cisplatin) [3,4]. Cisplatin, alone or in combination with other drugs, is used in chemotherapy against a large range of cancers, especially solid tumors [5–11]. The antineoplastic activity of cisplatin derivatives is related to interactions by covalent attachment to specific DNA sites, inducing conformational changes, inhibition of DNA transcription and, consequently, cell death by apoptosis [5,7,11]. Despite of the effectiveness of this class of compounds, many side effects, such as nephrotoxicity and hepatotoxicity, represent a strong restriction to the use of these compounds [10]. Therefore, there is a need for other therapeutic agents different from those of platinum in order to overcome the problems with cisplatin chemotherapy [12]. Among the candidates, ruthenium complexes present high potential to be used as metal based therapeutic agents, and some compounds like NAMI-A ([Him][trans-RuCl$_4$(DMSO)(im)], im = imidazole) and KP1019, ([Hind]-[trans-[RuCl$_4$(ind)$_2$], ind = indazole) have already been submitted

to phase II clinical tests [13]. Although their exact mechanism of action is still uncertain, some hypotheses suggest that, unlike the cisplatin derivatives, the primary target of ruthenium compounds is not the DNA, supporting the idea that these compounds might be active against cisplatin resistant tumors [14]. In fact, the pre-clinical trials of NAMI-A has shown a variety of mechanisms of action and should be considered as an anti-metastatic drug; however the toxicity profile and the lack of substantial efficacy results makes its future undefined [15]. Therefore, new ruthenium compounds with cytotoxic properties are still of interest.

N,N-Dialkyl-*N'*-acylthioureas (HRR[1]atu, Chart 1) and their metal complexes have attracted the attention of many researchers in the past few years due to their catalytic applications [16–18] and pharmacological activities such as antitumor [19–21], antibacterial [22], antimalarial [23], antifungal [24,25], herbicidal [26] as well as potential radiopharmaceutical agents [27–29]. They are versatile ligands with huge coordination chemistry. In most of the structurally characterized complexes they act as either monoanionic *O,S*-bidentate [17,19,20,23,25,28–33] or neutral *S*-monodentate ligands [18,21,34–39], while few examples neutral bidentate *N,S* [40] and monobasic bridging ligands, *O* and *S* bonded to M and *N* bonded to M' [41] or *O* and *S* bonded to M and *N,N'* bonded to M' [42], have been found. In the last case, the strategy used to access a dimeric complex was to include an additional donor atom in the periphery of the acylthiourea in other to connect Re(V) metal atoms [42]. Heteroleptic mono-chelate Ru(II) and homoleptic tris-chelate Ru(III) complexes containing acylthiourea ligands have already been reported [16–18,30,43]. However there are only two ruthenium complexes with full structural characterization: homoleptic tris-chelates of the type [Ru^{III}(R$_1$R$_2$atu)$_3$] (Chart 1A) [43] and organometallic ruthenium(II) complexes of the type [Ru^{II}Cl$_2$(η^6-*p*-cymene)(HR$_1$R$_2$atu)] (Chart 1B) [18] containing monodentate acylthiourea ligands (see Chart 1). To our knowledge, no heteroleptic tris-chelate Ru(II) complexes with acylthiourea have been reported in the literature.

In a previous paper we reported the synthesis, characterization and cytotoxic evaluation against tumor cells of ruthenium thiourea derivatives of the type *trans*-[Ru(PPh$_3$)$_2$(R$_1$R$_2$atu)(bipy)](PF$_6$) (Chart 1C) [44]. Their DNA and albumin binding ability was also evaluated. In the present paper, we describe the synthesis, spectroscopic and structural characterization of five new heteroleptic ruthenium(II) complexes containing three different classes of chelate ligands dppb, bipy and *N,N*-disubstituted-*N'*-acylthioureas, The two dppb and bipy ligands (see Chart 2) have been kept unchanged, while the thiourea residues have been modified throughout the experiments. The biological screening of these complexes for inhibitory effects against breast and prostate tumor cell lines and normal fibroblast cells is also reported. Furthermore,

a preliminary study by means of confocal microscopy was performed in order to have a highlight about the mechanism of action of these ruthenium complexes.

2. Experimental

2.1. Material and measurements

All manipulations were carried out under purified argon with standard Schlenk techniques. The solvents were reagent grade and were distilled and degassed according to standard procedures before use RuCl$_3$·3H$_2$O, 1,4-bis(diphenylphosphino)butane (dppb), and 2,2-bipyridine (bipy) were used as supplied by Sigma–Aldrich.

The *N,N*-disubstituted-*N'*-acylthioureas used as ligands in this work were synthesized by the procedure previously reported in the literature [19]. The ruthenium precursor *cis*-[RuCl$_2$(dppb) (bipy)] was prepared as reported earlier [45].

The IR spectra were recorded on a FTIR Bomem-Michelson 102 spectrometer in the 4000–200 cm^{-1} region using CsI pellets. Conductivity values were obtained using 1.0 mM solutions of the complexes in CH$_2$Cl$_2$, using a Meter Lab CDM2300 instrument. ^{1}H NMR spectra were recorded at 293 K, on a BRUKER 9.4 T spectrometer (400 MHz for hydrogen frequency) with internally referenced to TMS, chemical shift (δ), multiplicity (m), spin–spin coupling constant (*J*), integral (I). The CDCl$_3$ was used as solvent, unless mentioned. ^{31}P{^{1}H} NMR was acquired at 161.98 MHz, with CH$_2$Cl$_2$ as solvent, with a capillary containing D$_2$O (external reference 85% H$_3$PO$_4$).

Cyclic voltammetry experiments were carried out in CH$_2$Cl$_2$ solutions containing 0.10 M, Bu$_4$NClO$_4$ (TBAP) (Fluka Purum), with a Bioanalytical Systems Inc. BAS-100B/W electrochemical analyzer; the working and auxiliary electrodes were stationary Pt foils, and the reference electrode was Ag/AgCl in a Luggin capillary probe. Under these conditions, ferrocene is oxidized at 0.43 V (Fc$^+$/Fc). Partial elemental analyses were carried out on Department of Chemistry of the Federal University of São Carlos – UFSCar, in an instrument of CHNS staff EA 1108 of the FISONS.

2.2. Synthesis of N,N-dialkyl-N'-acylthioureas

A solution of an appropriate acyl chloride (30 mmol) in acetone (50 mL) was added dropwise to a suspension of KSCN (0.01 mol) in acetone (30 mL). To the resulting solution was added, slowly and with constant stirring, the corresponding amine (40 mmol) dissolved in acetone. The solution was cooled in an ice-water bath and the stirring was continued at room temperature for 2–9 h, until the reaction was completed (the reaction was monitored by TLC). The reaction mixture was then poured into 600 mL of cold
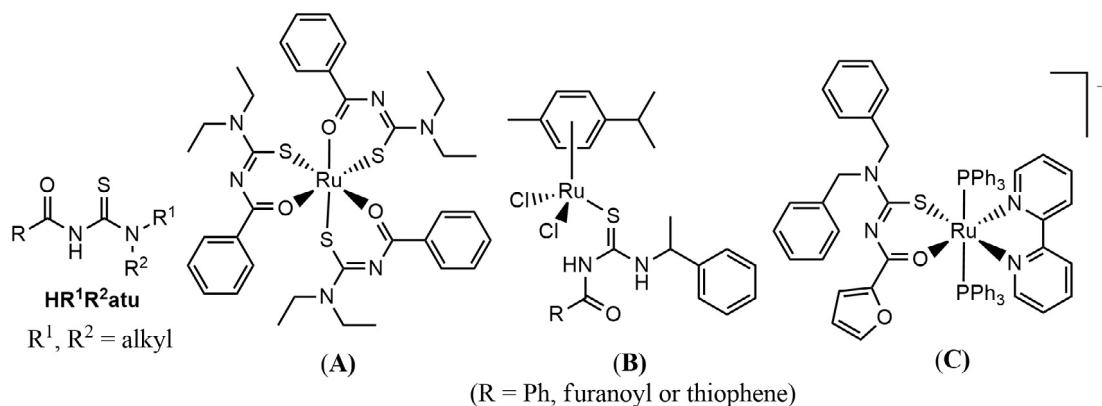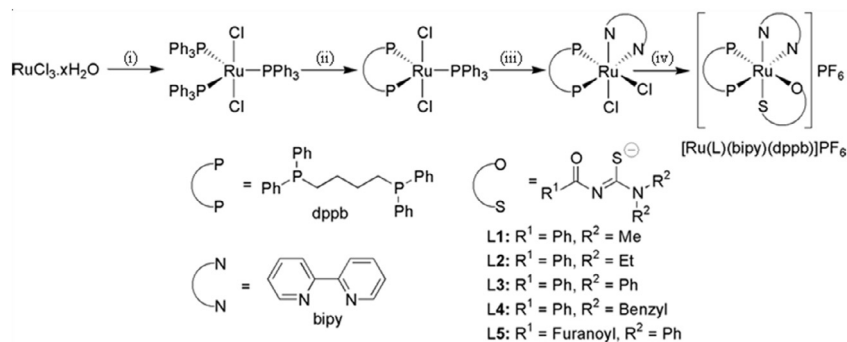

HR^{1}R^{2}atu

R^1, R^2 = alkyl

(A)   **(B)**   **(C)**

(R = Ph, furanoyl or thiophene)

Chart 1. *N,N*-Dialkyl-*N'*-acylthiourea ligands and their ruthenium complexes determined by X-ray studies.

Chart 2. Pathways for the synthesis of the [Ru^{II}(L)(dppb)(bipy)](PF$_6$) complexes. (i) CH$_3$OH, PPh$_3$ Δ; (ii) dppb, CH$_2$Cl$_2$; (iii) bipy, CH$_2$Cl$_2$; (iv) HL1–5, NH$_4$PF$_6$, MeOH, Δ.

water. The solid *N,N*-disubstituted-*N'*-acylthioureas were collected by filtration and finally purified by recrystallization from ethanol [19].

2.3. Synthesis of the complexes

The precursor *cis*-[Ru^{II}Cl$_2$(dppb)(bipy)] was prepared by reacting [Ru^{II}Cl$_2$(dppb)(PPh$_3$)] (0.663 mmol; 500.0 mg) with 2,2'-bipyridine (0.663 mmol; 103.5 mg) in dichloromethane, under an atmosphere of Ar. After 48 h of stirring under reflux, the solution was concentrated to ca. 2 mL and diethyl ether was added to precipitate a red solid. The solid was filtered off, washed well with diethyl ether (3 × 5 mL) and dried in vacuum for 24 h. Yield: 86% (430.1 mg). ^{31}P{^{1}H} NMR: δ(ppm) 39.6 (d, ^2J = 38.8 Hz), 31.6 (d, ^2J = 38.8 Hz).

The new complexes in study were synthesized from direct reactions of the precursor, *cis*-[Ru^{II}Cl$_2$(dppb)(bipy)], with the *N,N*-disubstituted-*N'*-acylthioureas, in methanol solutions (Chart 2). A solution of the corresponding *N,N*-dialkyl-*N'*-acylthiourea (0.133 mmol), dissolved in 30 mL of methanol, was added the precursor complex *cis*-[Ru^{II}Cl$_2$(dppb)(bipy)] (0.133 mmol). After 48 h of stirred under reflux, equimolar amount of NH$_4$PF$_6$ dissolved in 1.0 mL of methanol was added. The resultant solution was concentrated to ca. 2 mL and diethyl ether was added to precipitate a orange solid. The solid was filtered off and washed well with diethyl ether (3 × 5 mL) and dried in vacuum for 24 h. Yield: 81–90%.

[Ru^{II}(L^1)(dppb)(bipy)](PF$_6$) (**1**): Yield 82.7 (%). *Anal.* Calc. for C$_{48}$H$_{47}$F$_6$N$_4$OP$_3$RuS: C, 55.65; H, 4.57; N, 5.41; S, 3.10. Found: C, 56.27; H, 4.30; N, 4.99; S, 2.82%. Molar conductivity (1 × 10^{-3} M in CH$_2$Cl$_2$): 31.2 Ω^{-1} cm^2 mol^{-1}. IR (ν_{max}/cm^{-1}): 1515m ν(C=O), 841s ν(P—F); 557m δ(P—F); 505m, 517m ν(Ru—P); 434w ν(Ru—N), 413w ν(Ru—O); 382w ν(Ru—S). UV–Vis (CH$_2$Cl$_2$, 10^{-5} M): λ/nm (ε/M^{-1} cm^{-1}) 298 (48661), 426 (9059). ^{1}H NMR [CDCl$_3$: δ ppm (m, *J*, I, attribution)]: 1.40 (t, *J* = 12 Hz, 1H, CH$_2$ dppb), 1.92–2.09 (m, 2H, CH$_2$ dppb), 2.32–2.55 (m, 3H, CH$_2$ dppb), 2.97 (t, *J* = 11 Hz, 1H, CH$_2$ dppb), 3.09 (s, 3H, CH$_3$), 3.11 (s, 3H, CH$_3$), 3.25 (q, *J* = 11 Hz, 1H, CH$_2$ dppb), 6.33 (t, *J* = 8 Hz, 2H, bipy), 6.74 (t, *J* = 8 Hz, 2H, bipy), 6.93 (t, *J* = 7 Hz, 1H, Ph), 6.98 (t, *J* = 6 Hz, 1H, Ph), 7.10–7.50 (m, 18H, an overlap of aromatic protons of bipy and phenyl groups), 7.64 (t, *J* = 8 Hz, 2H, Ph), 7.78 (d, *J* = 8 Hz, 1H, Ph), 7.89 (t, *J* = 8 Hz, 2H, Ph), 8.16 (t, *J* = 8 Hz, 1H, Ph), 8.23 (d, *J* = 8 Hz, 1H, Ph), 8.57 (d, *J* = 6 Hz, 1H, Ph), 8.97 (d, *J* = 6 Hz, 1H, Ph). ^{31}P{^{1}H} NMR [CH$_2$Cl$_2$ (D$_2$O): δ (ppm)] 43.2 (d); 36.1 (d), $^2J_{P-P}$ = 31 Hz.

[Ru^{II}(L^2)(dppb)(bipy)](PF$_6$) (**2**): Yield 88.2 (%). *Anal.* Calc. for C$_{50}$H$_{51}$F$_6$N$_4$OP$_3$RuS: C, 56.44; H, 4.83; N, 5.27; S, 3.01. Found: C, 56.49; H, 4.99; N, 4.95; S, 2.78%. Molar conductivity (1 × 10^{-3} M in CH$_2$Cl$_2$): 29.2 Ω^{-1} cm^2 mol^{-1}. IR (ν_{max}/cm^{-1}):

1515 s ν(C=O), 839s ν(P—F), 557m δ(P—F); 507m, 517m ν(Ru—P), 436w ν(Ru—N), 411w ν(Ru—O), 378w ν(Ru—S). UV–Vis (CH$_2$Cl$_2$, 10^{-5} M): λ/nm (ε/M^{-1} cm^{-1}) 299 (41561), 426 (7079). ^{1}H NMR [CDCl$_3$: δ ppm (m, *J*, I, attribution)]: 1.04 (t, *J* = 7 Hz, 3H, CH$_3$), 1.24 (t, *J* = 7 Hz, 3H, CH$_3$), 1.48 (t, *J* = 12 Hz, 1H, CH$_2$ dppb), 1.83–1.99 (m, 2H, CH$_2$ dppb), 2.26–2.57 (m, 3H, CH$_2$ dppb), 3.03–3.19 (m, 2H, CH$_2$ dppb), 1.48 (d, *J* = 12 Hz, 1H, CH$_2$ dppb), 3.39–3.50 (m, 2H, CH$_2$CH$_3$), 3.61 (dq, ^2J = 13 Hz, ^3J = 7 Hz, 1H, CH$_2$CH$_3$), 3.77 (dq, ^2J = 13 Hz, ^3J = 7 Hz, 1H, CH$_2$CH$_3$), 6.46 (t, *J* = 8 Hz, 2H, bipy), 6.83 (t, *J* = 7 Hz, 2H, bipy), 6.92 (t, *J* = 7 Hz, 1H, Ph), 7.00 (t, *J* = 7 Hz, 1H, Ph), 7.07–7.55 (m, 20H, an overlap of aromatic protons of bipy and phenyl groups), 7.67 (d, *J* = 8 Hz, 1H, Ph), 7.92 (d, *J* = 8 Hz, 2H, Ph), 8.03–8.10 (m, 2H, Ph), 8.67 (d, *J* = 5 Hz, 1H, Ph), 8.88 (d, *J* = 6 Hz, 1H, Ph). ^{31}P{^{1}H} NMR [CH$_2$Cl$_2$ (D$_2$O): δ (ppm)] 43.2 (d); 36.6 (d), $^2J_{P-P}$ = 31 Hz.

[Ru^{II}(L^3)(dppb)(bipy)](PF$_6$) (**3**): Yield 85.4 (%). *Anal.* Calc. for C$_{58}$H$_{51}$F$_6$N$_4$OP$_3$RuS: C, 60.05; H, 4.43; N, 4.83; S, 2.76. Found: C, 60.43; H, 4.28; N, 4.58; S, 2.58%. Molar conductivity (1 × 10^{-3} M in CH$_2$Cl$_2$): 27.2 Ω^{-1} cm^2 mol^{-1}. IR (ν_{max}/cm^{-1}): 1515s ν(C=O), 839s ν(P—F), 557 δ(P—F); 505, 517m ν(Ru—P), 492m ν(Ru—N), 434w ν(Ru—O), 372w ν(Ru—S). UV–Vis (CH$_2$Cl$_2$, 10^{-5} M): λ/nm (ε/M^{-1} cm^{-1}) 299 (45616), 426 (8012). ^{1}H NMR [CDCl$_3$: δ ppm (m, *J*, I, attribution)]: 1.34 (t, *J* = 12 Hz, 1H, CH$_2$ dppb), 1.76–2.51 (m, 5H, CH$_2$ dppb), 2.92 (t, *J* = 10 Hz, 1H, CH$_2$ dppb), 3.06 (q, *J* = 10 Hz, 1H, CH$_2$ dppb), 6.31 (t, *J* = 8 Hz, 2H, bipy), 6.78 (t, *J* = 7 Hz, 2H, bipy), 6.95–6.43 (m, 31H, an overlap of aromatic protons of bipy and phenyl groups), 7.61 (t, *J* = 7 Hz, 1H, Ph), 7.82 (t, *J* = 8 Hz, 2H, Ph), 7.89 (d, *J* = 8 Hz, 1H, Ph), 8.15 (t, *J* = 8 Hz, 1H, Ph), 8.26 (d, *J* = 8 Hz, 1H, Ph), 8.63 (d, *J* = 6 Hz, 1H, Ph), 8.83 (d, *J* = 6 Hz, 1H, Ph). ^{31}P{^{1}H} NMR [CH$_2$Cl$_2$ (D$_2$O): δ (ppm)] 40.4 (d); 38.1 (d), $^2J_{P-P}$ = 31 Hz.

[Ru^{II}(L^4)(dppb)(bipy)](PF$_6$)·2H$_2$O (**4**): Yield 85.5 (%). *Anal.* Calc. for C$_{60}$H$_{57}$F$_6$N$_4$OP$_3$RuS·2H$_2$O: C, 58.77; H, 5.01; N, 4.57; S, 2.63%. Found: C, 58.70; H, 5.23; N, 4.63; S, 2.23%. Molar conductivity (1 × 10^{-3} M in CH$_2$Cl$_2$): 28.0 Ω^{-1} cm^2 mol^{-1}. IR (ν_{max}/cm^{-1}): 1516s ν(C=O), 841s ν(P—F), 505, 517m ν(Ru—P), 492m ν(Ru—N), 436w ν(Ru—O), 366w ν(Ru—S). UV–Vis (CH$_2$Cl$_2$, 10^{-5} M): λ/nm (ε/M^{-1} cm^{-1}) 298 (23291), 422 (2829). ^{1}H NMR [CDCl$_3$: δ ppm (m, *J*, I, attribution)]: 1.39 (t, *J* = 10 Hz, 1H, CH$_2$ dppb), 1.80 (t, *J* = 10 Hz, 2H, CH$_2$ dppb), 2.20–2.47 (m, 3H, CH$_2$ dppb), 2.97 (t, *J* = 11 Hz, 1H, CH$_2$ dppb), 3.16 (q, *J* = 11 Hz, 1H, CH$_2$ dppb), 3.63 (t, *J* = 11 Hz, 1H, CH$_2$ dppb), 4.75–5.07 (m, 4H, CH$_2$, benzyl), 6.23–6.32 (m, 3H, bipy), 6.46 (t, *J* = 3 Hz, 1H, bipy), 6.75–6.83 (m, 3H, bipy + Ph), 6.96 (t, *J* = 7 Hz, 1H, Ph), 7.03 (t, *J* = 7 Hz, 2H, Ph), 7.07–7.50 (m, 25H, an overlap of aromatic protons of bipy and phenyl groups), 7.64 (t, *J* = 8 Hz, 1H, Ph), 7.82 (d, *J* = 8 Hz, 2H, Ph), 7.96 (t, *J* = 8 Hz, 2H, Ph), 8.06 (t, *J* = 7 Hz, 1H, Ph), 8.14 (d, *J* = 8 Hz, 1H, Ph), 8.36 (d, *J* = 6 Hz, 1H, Ph), 8.71 (d, *J* = 6 Hz, 1H, Ph). ^{31}P{^{1}H} NMR [CH$_2$Cl$_2$ (D$_2$O): δ (ppm)] 43.8 (d); 36.7 (d), $^2J_{P-P}$ = 35 Hz.

$[Ru^{II}(L^5)(dppb)(bipy)](PF_6)$ (**5**): Yield 87.8 (%). *Anal.* Calc. for $C_{56}H_{49}F_6N_4O_2P_3RuS$: C, 56.71; H, 4.55; N, 4.72; S, 2.70. Found: C, 56.23; H, 5.03; N, 5.21; S, 2.92%. Molar conductivity (1×10^{-3} M in CH_2Cl_2): 29.9 Ω^{-1} cm^2 mol^{-1}. IR (ν_{max}/cm^{-1}): 1519sν(C=O), 841s ν(P—F), 505, 517m ν(Ru—P), 492m ν(Ru—N), 436w ν(Ru—O), 366w ν(Ru—S). UV–Vis (CH_2Cl_2, 10^{-5} M): λ/nm (ε/M^{-1} cm^{-1}) 298 (27 410). ^{1}H NMR [CDCl$_3$: δ ppm (m, J, I, attribution)]: 1.37 (m, 1H, CH$_2$ dppb), 1.85–2.03 (m, 2H, CH$_2$ dppb), 2.22–2.48 (m, 3H, CH$_2$ dppb), 2.92 (t, $J = 10$ Hz, 1H, CH$_2$ dppb), 3.18 (q, $J = 10$ Hz, 1H, CH$_2$ dppb), 6.08 (d, $J = 8$ Hz, 1H, bipy), 6.20 (d, $J = 7$ Hz, 1H, bipy), 6.31 (t, $J = 7$ Hz, 2H, bipy), 6.80 (t, $J = 7$ Hz, 2H, bipy), 7.00 (t, $J = 7$ Hz, 2H, bipy), 6.90–7.48 (m, 26H, an overlap of aromatic protons of furoyl, bipy and phenyl groups), 7.73 (t, $J = 7$ Hz, 1H, Ph), 7.84 (d, $J = 8$ Hz, 1H, Ph), 7.98 (t, $J = 8$ Hz, 2H, Ph), 8.04–8.13 (m, 2H, Ph), 8.64 (d, $J = 6$ Hz, 1H, Ph), 8.97 (d, J = 6 Hz, 1H, Ph). ^{31}P{^{1}H} NMR [CH$_2$Cl$_2$ (D$_2$O): δ (ppm)] 40.2 (d); 37.7 (d), $^2J_{P-P} = 31$ Hz.

2.4. Crystal structure determination

Single crystals suitable for X-ray diffraction were obtained by slow evaporation of CH$_2$Cl$_2$ solutions of **1** at room temperature. The data collection was performed using Mo Kα radiation ($\lambda = 71.073$ pm) on a BRUKER APEX II Duo diffractometer. Standard procedures were applied for data reduction and absorption correction. The structures were solved with SHELXS97 using direct methods [46] and all non-hydrogen atoms were refined with anisotropic displacement parameters with SHELXL2014 [47]. The hydrogen atoms were calculated at idealized positions using the riding model option of SHELXL2014 [47]. Hexafluorophosphate anion and phenyl ring of the thiourea ligand are disordered and were refined over two sites with occupancies 0.636:0.364 and 0.466:0.534, respectively. Table 1 contains more detailed information about the structure determinations.

Table 1
Crystal data and structure refinement details for $[Ru^{II}(L^1)(dppb)(bipy)](PF_6)$ (**1**).

	1
Empirical formula	$C_{48}H_{47}F_6N_4OP_3RuS$
Formula weight	1035.94
T (K)	296(2)
λ (Å)	0.71073
Crystal system	monoclinic
Space group	$P2_1/c$
Unit cell dimensions	
a (Å)	12.1677(6)
b (Å)	28.1703(14)
c (Å)	14.4942(8)
β (°)	109.5400(10)
V (Å^3)	4682.0(4)
Z	4
D_{calc} (Mg/m^3)	1.470
Absorption coefficient (mm^{-1})	0.547
Crystal size (mm)	$0.70 \times 0.68 \times 0.25$
θ range for data collection (°)	1.45–25.04
Index ranges	$14 \leqslant h \leqslant 14$, $-30 \leqslant k \leqslant 33$, $-16 \leqslant l \leqslant 17$
Reflections collected	28 202
Independent reflections (R_{int})	8212 (0.0175)
Completeness to theta $\theta = 25.044°$	98.9%
Absorption correction	multi-scan
Maximum and minimum transmission	0.7452 and 0.6737
Refinement method	full-matrix least-squares on F^2
Data/restraints/parameters	8212/103/641
Goodness-of-fit (GOF) on F^2	1.050
Final R indices [$I > 2\sigma(I)$]	$R_1 = 0.0260$, $wR_2 = 0.0643$
R indices (all data)	$R_1 = 0.0291$, $wR_2 = 0.0661$
Residual maximum and minimum (e Å^{-3})	0.363 and −0.378
CCDC number	1418917

2.5. Cell culture assay

The *in vitro* cytotoxicity assays on cultured human tumor cell lines still represent the standard method for the initial screening of antitumor agents. Thus, as a first step to assess their pharmacological properties, the ruthenium complexes were assayed toward human breast tumor cells MCF-7 (ATCC: HTB-22), human prostate tumor cells DU-145 (ATCC:HTB-81) and against from mouse L929 fibroblast cells (ATCC:CCL 1). The cells were routinely maintained with Dulbecco's Modified Eagle's medium (DMEM-for L929 and DU-145) or RPMI 1640 (for MCF-7) supplemented with 10% fetal bovine serum (FBS), at 37 °C in a humidified 5% CO$_2$ atmosphere. For the cytotoxicity assay, 1.5×10^4 cells well^{-1} were seeded in 200 µL of complete medium in 96-well plates (Corning Costar). The complex was dissolved in sterile DMSO (from 10 to 0.01 mM). One microliter of each complex sample was added to 200 µL medium. Cells were exposed to the complex for a 48 h-period. The conversion of MTT to formazan by metabolically viable cells was monitored by an automated microplate reader at 540 nm.

2.6. Confocal fluorescence microscopy studies

In order to characterize the morphology of the cytoskeletal and of the cell nucleus green and blue fluorescence of Alexa Fluor 488 Phalloidin and DAPI, respectively, were used to mark the cellular localization. The DU-145 cells were seeded into 24 wells cell culture cluster at the density of 0.35×10^5 per well (1 mL, 5% CO$_2$, 37 °C). After 24 h, the cells were treated with 0.14 µM of complex **5** (IC$_{50}$ value), and control cell was treated with DMSO and incubated for 24 h. The treated and control cells were washed twice in PBS (phosphate-buffered saline, pH 7.4) and fixed with a solution of 3.7% formaldehyde in PBS for 2 h, washed 2× in PBS (5 min), permeabilized with triton-x 0.1% for 20 min and washed again with PBS (2 times for 5 min). The material was incubated with the "Alexa Fluor 488 Phalloidin" solution (5 µL of the stock solution "Alexa Fluor 488 Phalloidin" + 200 µL of PBS + 2 µL of BSA) for 30 min and washed 2× with PBS (5 min each). After that, the material was marked with the DAPI solution (30 nM) for 5 min and washed 2× with PBS (5 min each). Finally, the material was mounted by using a montage ProLong® Gold reagent (Molecular Probes) and analyzed in a Laser Leica TCS SP5II Confocal Microscopy. The wavelength of the laser was 488 nm for the actin (Alexa Fluor 488 Phalloidin) and 305 nm for the nucleus (DAPI).

3. Results and discussion

The Chart 2 shows the pathway for the synthesis of the Ru(II) complexes. The complexes were obtained by reacting methanolic solutions of acylthioureas with the *cis*-dichlorido(1,4-bis (diphenylphosphino)butane)(2,2′-bipyridine)ruthenium(II) precursor, *cis*-[Ru^{II}Cl$_2$(dppb)(bipy)]. The coordination between the acylthiourea derivatives and the precursor proceeded by an exchange reaction, which involved deprotonation of the acylthioureido group of the ligands upon complexation [19]. The orange complexes were obtained using Schlenk techniques under an atmosphere of argon. Elemental analyses of the complexes suggest the formation of *cis*-[Ru^{II}(L)(dppb)(bipy)](PF$_6$) (**1–5**) (Chart 2). The compounds are air stable and very soluble in chlorinated solvents, acetone, and methanol but are virtually insoluble in hydrocarbon solvents, diethyl ether and water.

3.1. Spectroscopic characterization

The infrared spectra of all compounds are in agreement with the proposed molecular formulas. The IR spectra of the ligands

show broad, strong absorptions in the range of 3050–3260 cm^{-1} occurs due to NH stretching vibration [19]. The coordination of the metal center to the carbonyl group decreases the C=O stretching vibration frequency by c.a. 180 cm^{-1}, when compared with the free ligands, in agreement with literature [48]. As observed, the asymmetric and symmetric N—H stretching vibration bands, presented in the free ligands, are absent in the IR spectra of the complexes. For all the complexes the ν(C=O) stretching vibration is found close to 1585 cm^{-1}. The ν(C=S) stretching vibrations, observed at 815–878 cm^{-1} in the spectra of free *N,N*-disubstituted-*N'*-acylthioureas, shift to the 734–769 cm^{-1} range in the complexes, indicating coordination through the sulfur atom of the ligands. This substantial change is an indication of deprotonation of the ligands and formation of a C—S single bond [49]. The absorptions at 515 and 437 cm^{-1} in the IR spectra of the complexes can be assigned to the Ru—P and Ru—O vibration mode, respectively [50]. The low-frequency region in the IR spectra of the complexes (**1**–**5**) shows low intensity bands, which could be assigned as Ru-S stretching vibrations [50]. Electronic spectra showed band in the UV region (299 nm) assigned to intraligand $\pi \to \pi^*$ transitions, also observed in the free ligands (dppb and bipy). The other band, observed as a shoulder band around 425 nm, is assigned to charge transfer from Ru(II) to the ligands [45].

The NMR (^{1}H and ^{31}P{^{1}H}) spectra of the complexes were carried out in order to elucidate the coordination of acylthiourea ligands with the *cis*-[Ru^{II}Cl$_2$(dppb)(bipy)] precursor. A comparative analysis was made on the basis of the spectroscopic data corresponding to both free and coordinated ligands.

The new Ru(II) complexes showed similar {^{1}H}-chemical shift pattern. Some hydrogen atom values of δ were not observed precisely due to overlapping of aromatic signals of dppb, bipy and thiourea ligands, however the ^{1}H NMR integrations and signal multiplicities are in agreement with the proposed structures. The ^{1}H NMR spectra of the free ligands showed basically three sets of well separated signals corresponding to their R$_1$, R$_2$ substituents and to the NH proton. The signals of the NH protons appear as broad singlets in the region between δ 8.35–8.80 ppm. Upon coordination the N—H proton signal disappears in accord with the deprotonation of the ligands as indicated by the IR spectra of the complexes [17,19,21,30].

The ^{31}P{^{1}H} NMR spectrum of the precursor *cis*-[Ru^{II}Cl$_2$(dppb)(bipy)] [18] in CH$_2$Cl$_2$ solution shows two doublets signals for the phosphorous donor atoms at 43.5 ppm and 29.8 ppm ($^2J_{P-P}$ = 32.9 Hz). The ^{31}P{^{1}H} NMR spectra of the compounds **1**–**5** showed doublets indicating the formation of unsymmetrical structures and the nonequivalency of the phosphorus atoms of the dppb ligand. Besides a septet at approximately –145.0 ppm were observed due to the PF$_6^-$ counter ion, according with the molar conductivity measurements for all compounds (see Section 2). The chemical shifts for complexes under study are similar, indicating that the magnetic shielding of the phosphorus atoms are very close, as expected, since they are *trans* to a nitrogen and the carbonyl oxygen atoms from the bipy and thiourea ligands, respectively.

3.2. Crystal structures

The structure of the complex **1** was studied by X-ray diffraction. The ORTEP representation of the representative complex along with the numbering scheme is presented in Fig. 1. Selected data of interatomic distances and main angles can be found in Table 2. The heteroleptic ruthenium(II) complex exhibits a 6-coordinated metal center bonded to the diphosphine (dppb), the bipyridine (bipy) and to the monoanionic thiourea L$^-$ ligand in *O,S*-bidentate mode, leading to a distorted octahedral geometry around the metal center. The ruthenium(II) charge is compensated by the PF$_6^-$
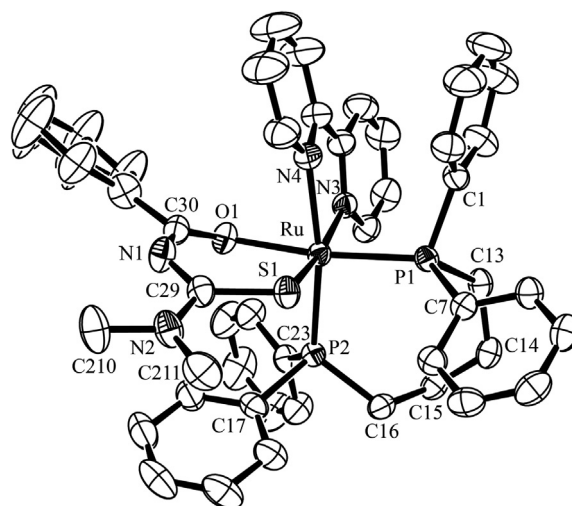

Fig. 1. ORTEP plot of complex **1** with the thermal ellipsoids at the 50% probability level. Hydrogen atoms, PF$_6^-$ and some atom labels are omitted for clarity. Phenyl ring of the thiourea ligand is disordered over two sites (occupancy 46.6:53.4).

Table 2
Selected bond lengths (Å) and angles (°) refined from X-ray for **1**.

	1
Bond lengths	
Ru–O(1)	2.1165(13)
Ru–S(1)	2.3595(5)
Ru–N(3)	2.1247(16)
Ru–N(4)	2.1489(17)
Ru–P(1)	2.2932(5)
Ru–P(2)	2.3069(5)
S(1)–C(29)	1.735(2)
O(1)–C(30)	1.269(2)
N(1)–C(30)	1.318(3)
N(1)–C(29)	1.339(3)
Bond angles	
P(1)–Ru–P(2)	95.358(18)
O(1)–Ru–N(3)	87.36(6)
O(1)–Ru–N(4)	79.10(6)
O(1)–Ru–P(1)	172.42(4)
O(1)–Ru–P(2)	90.33(4)
O(1)–Ru–S(1)	91.15(4)
N(3)—Ru–S(1)	168.74(5)
N(4)–Ru–S(1)	91.52(6)
P(1)–Ru–S(1)	93.809(18)
P(2)–Ru–S(1)	90.477(19)
C(29)–S(1)–Ru	107.25(7)
C(30)–O(1)–Ru	126.90(13)

counter ion, forming a monocationic complex. The coordination of the dppb, bipy and thiourea ligands forms a seven-, five- and six-membered chelate rings, respectively. The negative charge of the monoanionic thiourea is delocalized over the ligand moiety, through the conjugated double bonds system, consistent with the single bond predominant character for the S—C bond (1.70–1.73 Å) and to the considerable double bond character observed for the C=N (around 1.33 Å) and C=O (around 1.27 Å) distances.

The sulfur atom of the acylthiourea ligand coordinates *trans* to the bipy nitrogen atom N3, while the oxygen atom O1 is *trans* coordinated to the phosphorous atom P1. The Ru—P, Ru—N, Ru—O and Ru—S bond lengths are in the expected range observed in similar Ru(II) compounds [51–54]. Furthermore, the bidentate ligands are almost perpendicular to each other, with P(2)—Ru(1)—S(1) and O(1)—Ru(1)—P(2) close to 90°. The P(1)—Ru—S(1) angle around 101° shows a clear distortion of the octahedral geometry. As

Table 3
Cyclic voltammograms (mV) of the complexes (**1**–**5**) (1.0 mM) in CH$_2$Cl$_2$ (Ag/AgCl, 0.1 mol/L PTBA, 100 mV/s).

Compound	Ru^{II}/Ru^{III} (E_{pa}) (mV)	$E_{1/2}$ (mV)	I_{pa}/I_{pc}
1	1036	930	0.97
2	940	890	1.02
3	994	941	0.95
4	1037	929	0.95
5	981	–	–

expected, no classical hydrogen bonds are found in the crystalline structures of the compounds.

3.3. Cyclic voltammetry

In order to investigate the redox behavior and the stability of the complexes in solution the cyclic voltammograms were recorded in dichloromethane at room temperature at the potential range 0 to +1.5 V with a Pt disc electrode *versus* an Ag/AgCl reference electrode. The complexes **1**–**4** showed quasi-reversible ($I_{pa}/I_{pc} \approx 1$) waves whose processes correspond to the one-electron oxidation of Ru(II) to Ru(III) (Table 3). The anodic peak around $E_{pa} = 1.0$ V is attributed to the oxidation of the ruthenium(II) ion to ruthenium(III) [18], while the complex **5** showed an irreversible process. In the case of complex **1**, a process related to the reduction of the thiourea ligand was also observed at 1190 mV.

The complexes presented cathodic peaks in the potential range from 940 to 1037 mV, showing that the substitution of the peripheral groups in the thiourea moiety (R1 and R2 groups) influences the electronic character of the ligands. When compared to the precursor *cis*-[Ru^{II}Cl$_2$(dppb)(bipy)] ($E_{1/2} = 650$ mV) [18], the oxidation potential of the thiourea derivatives presented a significant increase. The higher redox potential observed for these complexes evidences a greater stability of the complexes upon coordination of

Table 4
Cytotoxic effect (IC$_{50}$) of **1**–**5** complexes and cisplatin against MCF-7, DU-145 and L929 (fibroblast cells), after 48 h of incubation.

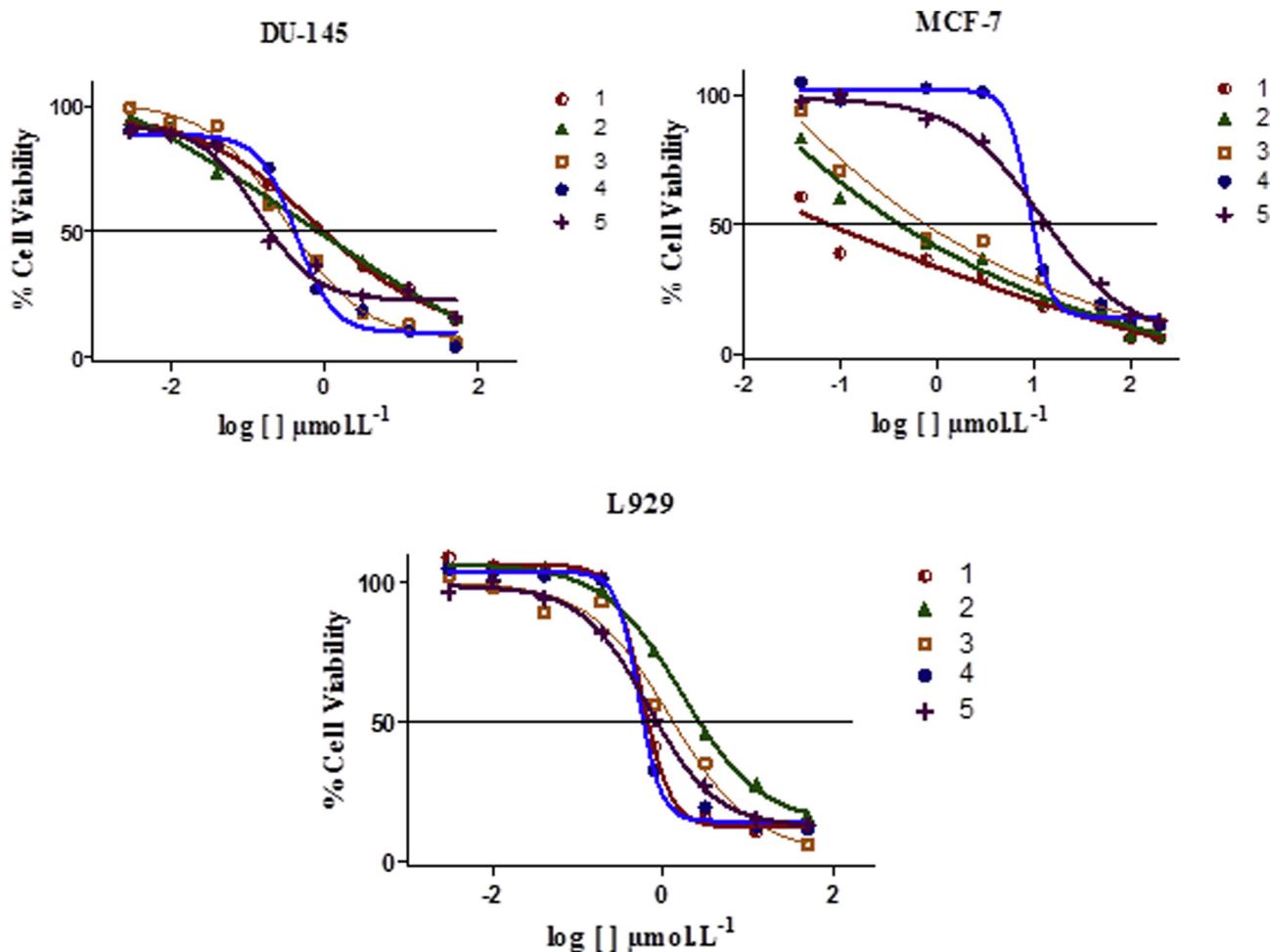| Complexes	L929 (μM)	MCF-7 (μM)	SI (IC$_{50L929}$/IC$_{50MCF-7}$)	DU-145 (μM)	SI (IC$_{50L929}$/IC$_{50DU-145}$)
(1)	0.57 ± 0.03	>0.10	>5.7	0.75 ± 0.21	0.76
(2)	1.65 ± 0.40	>0.10	>16.5	1.75 ± 0.45	0.94
(3)	1.22 ± 0.41	>0.10	>12.2	0.31 ± 0.06	3.93
(4)	0.52 ± 0.06	8.90 ± 1.95	0.06	0.42 ± 0.07	1.24
(5)	0.66 ± 0.06	12.21 ± 2.15	0.05	0.14 ± 0.04	4.71
Cisplatin	16.53 ± 2.38	2.43 ± 0.20	6.80	2.00 ± 0.47	8.27

Fig. 2. Effects of *N*-disubstituted-*N'*-acylthiourea ruthenium complexes on the DU-145, MCF-7 and L929 cells proliferation.

the thiourea ligands. Finally, a second reduction process was observed after the first anodic scan which was attributed to a reduction process of the thiourea ligand.

3.4. Cytotoxicity assays

The cytotoxicities of all five complexes were evaluated against two human tumor cell lines representing tumors of two different origins, prostate and breast, in addition to a mouse fibroblast cell line, by means of the colorimetric MTT assay. They were compared to cisplatin and free ligands under the same conditions. Cell respiration, as an indicator of cell viability, was determined by the mitochondrial dependent reduction of MTT (3-(4,5-dimethylthiazol-2-yl)-2,5-diphenyltetrazolium bromide) to formazan [55].

The percentage of cell viability was calculated by dividing the average absorbance of the cells treated with the ruthenium complex by that of the control; percentage of cell viability *versus* drug concentration (logarithmic scale) was plotted to determine the IC_{50} (drug concentration at which 50% of the cells are viable relative to the control), with its estimated error derived from the average of 3 trials. The concentrations that produce 50% of growth inhibition (IC_{50}, μM) are shown in Table 4, calculated from the dose-survival curves obtained after drug treatment represented in the Fig. 2.

The compound 5 was the most effective compound against human prostate tumor cell (DU-145) line with IC_{50} value of 0.14 μM, while the compounds 1–3 presented the same IC_{50} value for the breast tumor cell line (MCF-7) >0.10 μM. All complexes presented significant cytotoxic effects with higher activity with respect to their uncoordinated acylthiourea, emphasizing the importance of the presence of the metal for antitumor biological activity presented by the new complexes, a different result from that observed for rhenium(V) complexes where the replacement of the halide by the chelating benzoylthiourea lead to a significant decrease of the biological activity [28]. This fact indicates different mechanisms for the biological activities of the uncoordinated acylthioureas and their related ruthenium(II) complexes. In order to determine the selectivity and to estimate the therapeutic window of the compounds presented here we also measured their cytotoxicity against fibroblast cells. With these results, it's possible to calculate the selectivity index (SI, relative activity of a compound against the tumor cell line compared with its cytotoxicity to normal cells) of each compound by the ratio of IC_{50} (fibroblast cells) to IC_{50} (tumor cells). The complexes 2 and 3 were found to

be the most selective for MCF-7 and DU-145 cell lines, respectively, (SI values around 17 and 4, respectively). Under an inverted microscope, cell shape and changes in it can be observed clearly. As shown in Fig. 3, DU-145 prostate tumor cells appeared epithelial cell morphology in the control group and there were very few round cells. Cells treated with 5 showed obvious morphological changes after the first 24 h; cells treated for 48 h showed, in addition to morphological changes, a loss of adhesion, an epithelial form and confluence, indicating the possibility of apoptosis [56].

Recently, our research group reported four ruthenium(II) complexes containing bistriphenylphosphines, bipyridine and N',N'-(disubstituted)-N'-acylthiourea ligands and their cytotoxicity against DU-145 tumor cells was in the range of 0.22–0.46 μM [44], in the present report the IC_{50} values are in the range of 0.14–1.75 μM, very similar to that observed for ruthenium-bis (triphenylphosphine). Interestingly, all complexes were more cytotoxic than cisplatin in the human DU-145 cell line.

3.5. Confocal fluorescence microscopy studies

The results indicate that the combination of Ru(II) and acylthiourea in a single molecule results in complexes that are more cytotoxic than the individual components alone, displaying in all cases low IC_{50} values and higher selectivity indexes. After verifying that these ruthenium complexes present remarkable cytotoxicity against DU-145 cells it is worth to investigate their mechanism of action. Given the higher selectivity of complex 5 against this tumor cell line, it was selected for a preliminary mechanism study. Thus we inspected morphological changes of the human prostate tumor cells DU-145 by confocal microscopy upon treatment with $[Ru^{II}(L^5)(dppb)(bipy)](PF_6)$ (Fig. 3). In control cells (Fig. 4A–C) the tubular aspect of the actin filaments (in green) were maintained after 24 h while the tumor cells incubated with $[Ru^{II}(L^5)(dppb) (bipy)](PF_6)$ (Fig. 4D–F) presented several damage due to fragmentation of the microfilaments after that time, in accord with cell death. The cell nucleus was also showed alterations in its morphology but in a much lower degree. When compared to the nucleus of the DU-145 control cells (Fig. 4A–C), the appearance of nucleus of the tumor cells treated with $[Ru^{II}(L^5)(dppb)(bipy)](PF_6)$ is only a bit different, indicating that the interaction of the ruthenium(II) complex with this organelle is quite weak. These results support the conclusion that the compounds are effective to cause cell death by causing modifications to the actin filaments which are
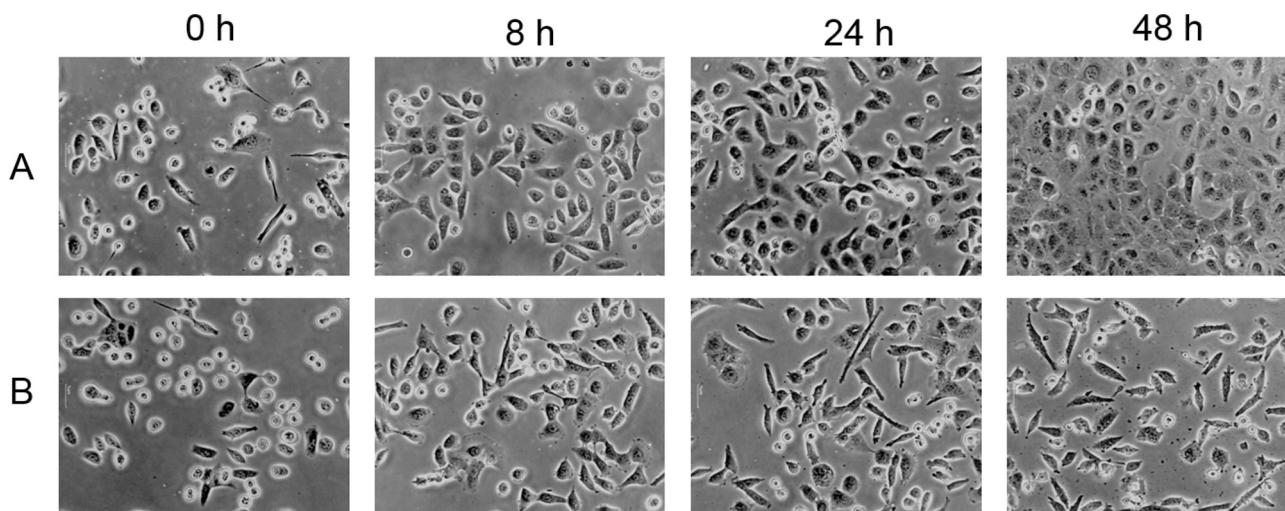
Fig. 3. Morphological study under an inverted microscope of DU-145 control cells (A) and cells treated with the IC_{50} value of complex 5 (B). The images are representative of pictures taken in three independent experiments ($n = 3$).
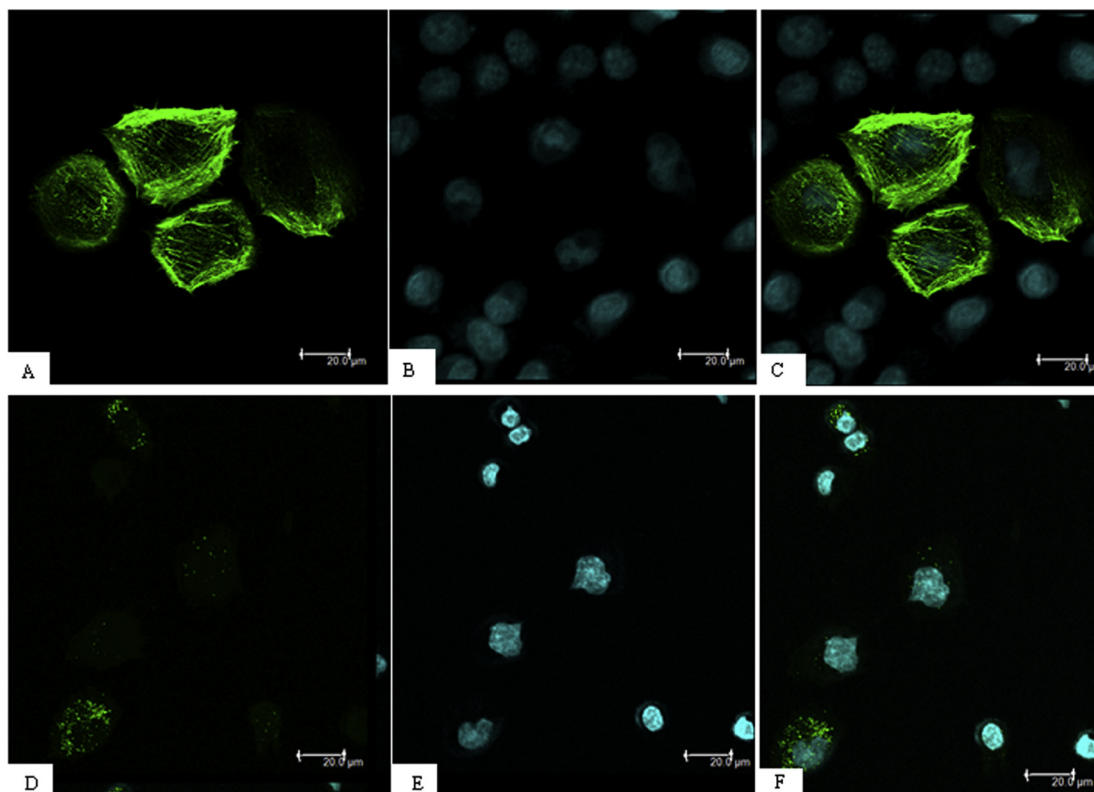
Fig. 4. Confocal fluorescence images (Alexa Fluor® 488 Phalloidin) of Actin-F (in green) + DAPI nuclear stain (in blue) upon 24 h of incubation. A–C are DU-145 control cells and D-F are DU-145 tumor cells treated with IC_{50} value of $[Ru^{II}(L^5)(dppb)(bipy)](PF_6)$ (**5**). (Colour online.)

cytoskeletal components responsible for normal cellular division. These results are similar to the presented by NAMI-A, for which interactions with actin proteins on the cell surface or with collagens of the extracellular matrix have been proposed as possible mechanisms of the anti-metastatic action [57]. Rhodium complexes also target cellular organelles rather than the nucleus [58]. Further experiments are necessary to comprehend the observed results and fully understand the mechanism of action of these compounds.

4. Conclusions

Heteroleptic tris-chelate ruthenium(II) complexes containing acylthiourea ligands can be prepared in high yields and purity. The cytotoxic behavior of some of the compounds under study is remarkable. The changes of peripheral groups R1 and R2 of the thiourea moiety influences the degree of cytotoxicity and complexation with ruthenium(II) metal center increases the activity in most cases, indicating that the metal center plays a key role on the activity. Further experiments are necessary to comprehend the observed results. The confocal microscopy images demonstrated that modifications of the actin filaments and consequently to the cytoskeletal might be responsible for the activity of these complexes instead of interaction with the nucleus.

Acknowledgements

Appendix A. Supplementary data

CCDC 1418917 contains the supplementary crystallographic data for complex **1**. These data can be obtained free of charge via http://www.ccdc.cam.ac.uk/conts/retrieving.html, or from the Cambridge Crystallographic Data Center, 12 Union Road, Cambridge CB2 1EZ, UK; fax: (+44) 1223-336-033; or e-mail: deposit@ccdc.cam.ac.uk. Supplementary data associated with this article can be found, in the online version, at http://dx.doi.org/10.1016/j.poly.2017.01.002.

References

[1] American Cancer Society. http://www.cancer.org/index, (accessed on 12.9.2016).
[2] G.I. Evan, K.H. Vousden, Nature 411 (2001) 342.
[3] B. Rosenberg, L.V. Camp, E.B. Grimley, J. Thomson, J. Biol. Chem. 242 (6) (1967) 1347.
[4] B. Rosenberg, L. VanCamp, J.E. Trosko, V.H. Mansour, Nature 222 (1969) 385.
[5] M. Fanelli, M. Formica, V. Fusi, L. Giorgi, M. Micheloni, P. Paoli, Coord. Chem. Rev. 310 (2016) 41.
[6] S. Ano, Z. Kuklenyik, L. Marzilli, B. Lippert, Cisplatin: Chemistry and Biochemistry of a Leading Anticancer Drug, VHCH-Wiley-VCH, Basel, 1999.
[7] F. Trudu, F. Amato, P. Vañhara, T. Pivetta, E.M. Peña-Méndez, J. Havel, J. Appl. Biomed. 13 (2015) 79.
[8] N.P.E. Barry, P.J. Sadler, Pure Appl. Chem. 86 (2014) 1897.
[9] P.J. Dyson, G. Sava, Dalton Trans. 16 (2006) 1929–Tr1933.
[10] L. Kelland, Nat. Rev. Cancer 7 (8) (2007) 573.
[11] J. Reedijk, Eur. J. Inorg. Chem. 2009 (10) (2009) 1303.
[12] P.I.S. Maia, V.M. Deflon, A. Ulrich, Future Med. Chem. 6 (13) (2014) 1515.
[13] B.M. Blunden, A. Rawal, H. Lu, M.H. Stenzel, Macromolecules 47 (5) (2014) 1646.
[14] C.R. Cardoso, M.V.S. Lima, J. Cheleski, E.J. Peterson, T. Venâncio, N.P. Farrell, R.M. Carlos, J. Med. Chem. 57 (11) (2014) 4906.
[15] S. Leijen, S.A. Burgers, P. Baas, D. Pluim, M. Tibben, E. van Werkhoven, E. Alessio, G. Sava, J.H. Beijnen, J.H.M. Schellens, Invest. New Drugs 33 (2015) 201.
[16] S. Amirnejat, F. Movahedi, H. Masrouri, M. Mohadesi, M.Z. Kassaee, J. Mol. Catal. A: Chem. 378 (2013) 135.

[17] N. Gunasekaran, N. Remya, S. Radhakrishnan, R. Karvembu, J. Coord. Chem. 64 (3) (2011) 491.

[18] M.M. Sheeba, M.M. Tamizh, L.J. Farrugia, A. Endo, R. Karvembu, Organometallics 33 (2) (2014) 540.

[19] A.M. Plutín, R. Mocelo, A. Alvarez, R. Ramos, E.E. Castellano, M.R. Cominetti, A.A. Batista, J. Inorg. Biochem. 134 (2014) 76.

[20] N. Selvakumaran, A. Pratheepkumar, S.W. Ng, E.R.T. Tiekink, R. Karvembu, Inorg. Chim. Acta 404 (2013) 82.

[21] N. Selvakumaran, S.W. Ng, E.R.T. Tiekink, R. Karvembu, Inorg. Chim. Acta 376 (1) (2011) 278.

[22] A. Saeed, M.S. Khan, H. Rafique, M. Shahid, J. Iqbal, Bioorg. Chem. 52 (2014) 1.

[23] T.J. Egan, K.R. Koch, P.L. Swan, C. Clarkson, D.A.V. Schalkwyk, P.J. Smith, J. Med. Chem. 47 (11) (2004) 2926.

[24] R.D. Campo, J.J. Criado, E. García, M.R. Hermosa, A. Jiménez-Sánchez, J.L. Manzano, F. Sanz, J. Inorg. Biochem. 89 (1–2) (2002) 74.

[25] R.D. Campo, J.J. Criado, R. Gheorghe, F.J. González, M.R. Hermosa, F. Sanz, E. Rodríguez-Fernández, J. Inorg. Biochem. 98 (8) (2004) 1307.

[26] M. Wang, L. Sun, F. Wan, L. Jiang, J. Pest. Sci. 37 (1) (2012) 15.

[27] N.H. Huy, U. Abram, Inorg. Chem. 46 (13) (2007) 5310.

[28] P.I.S. Maia, H.H. Nguyen, A. Hagenbach, S. Bergemann, R. Gust, V.M. Deflon, U. Abram, Dalton Trans. 42 (14) (2013) 5111.

[29] H.H. Nguyen, J.J. Jegathesh, P.I.S. Maia, V.M. Deflon, R. Gust, S. Bergemann, U. Abram, Inorg. Chem. 48 (19) (2009) 9356.

[30] S. Pisiewicz, J. Rust, C.W. Lehmann, F. Mohr, Polyhedron 29 (8) (2010) 1968.

[31] B. O'Reilly, A.M. Plutín, H. Pérez, O. Calderón, R. Ramos, R. Martínez, N. Martín, Polyhedron 36 (1) (2012) 133.

[32] H. Mandal, D. Ray, Inorg. Chim. Acta 414 (2014) 127.

[33] S.S. Tan, A.A. Al-abbasi, M.I.M. Tahir, M.B. Kassim, Polyhedron 68 (2014) 287.

[34] M. Iliş, M. Micutz, F. Dumitraşcu, I. Pasuk, Y. Molard, T. Roisnel, V. Cîrcu, Polyhedron 69 (2014) 31.

[35] R.C. Luckay, F. Mebrahtu, C. Esterhuysen, K.R. Koch, Inorg. Chem. Commun. 13 (4) (2010) 468.

[36] B. Schmitt, T.I.A. Gerber, E. Hosten, R. Betz, Inorg. Chem. Commun. 24 (2012) 136.

[37] N. Gunasekaran, S.W. Ng, E.R.T. Tiekink, R. Karvembu, Polyhedron 34 (1) (2012) 41.

[38] N. Gunasekaran, P. Ramesh, M.N.G. Ponnuswamy, R. Karvembu, Dalton Trans. 40 (46) (2011) 12519.

[39] A.N. Westra, S.A. Bourne, C. Esterhuysen, K.R. Koch, Dalton Trans. 12 (2005) 2162.

[40] K.R. Koch, Coord. Chem. Rev. 216–217 (2001) 473.

[41] G. Kemp, A. Roodt, W. Purcell, K.R. Koch, Dalton Trans. 23 (1997) 4481.

[42] H.H. Nguyen, U. Abram, Inorg. Chem. Commun. 11 (12) (2008) 1478.

[43] J. Sieler, R. Richter, E. Hoyer, L. Beyer, O. Lindqvist, L. Andersen, Z. Anorg. Allg. Chem. 580 (1) (1990) 167.

[44] R.S. Correa, K.M. de Oliveira, F.G. Delolo, A. Alvarez, R. Mocelo, A.M. Plutin, M.R. Cominetti, E.E. Castellano, A.A. Batista, J. Inorg. Biochem. 150 (2015) 63.

[45] S.L. Queiroz, A.A. Batista, G. Oliva, M.T.P. Gambardella, R.H.A. Santos, K.S. MacFarlane, B.R. James, Inorg. Chim. Acta 267 (2) (1998) 209.

[46] G.M. Sheldrick, SHELXS97, Program for the Solution of Crystal Structures, University of Göttingen, Germany, 1997.

[47] G.M. Sheldrick, SHELXL2014, Program for the Refinement of Crystal Structures, University of Göttingen, Germany, 2014.

[48] M. Mikami, I. Nakagawa, T. Shimanouchi, Spectrochim. Acta Part A Mol. Biomol. Spectrosc. 25 (2) (1969) 365.

[49] C. Rodrigues, A.A. Batista, R.Q. Aucélio, L.R. Teixeira, L.C. Visentin, H. Beraldo, Polyhedron 27 (14) (2008) 3061.

[50] K. Nakamoto, Infrared and raman spectra of inorganic and coordination, fourth ed., Compounds, Wiley, New York, 1986.

[51] M.I.F. Barbosa, E.M.A. Valle, S.L. Queiroz, J. Ellena, E.E. Castellano, V.R.S. Malta, A.A. Batista, Polyhedron 29 (11) (2010) 2297.

[52] K. Wohnrath, M.P. de Araujo, L.R. Dinelli, A.A. Batista, I.S. Moreira, E.E. Castellano, J. Ellena, J. Chem. Soc., Dalton Trans. 19 (2000) 3383.

[53] M.O. Santiago, C.L.D. Filho, I.S. Moreira, R.M. Carlos, S.L. Queiroz, A.A. Batista, Polyhedron 22 (24) (2003) 3205.

[54] K. Wohnrath, A.A. Batista, A.G. Ferreira, J. Zukerman-Schpector, L.A.A. de Oliveira, E.E. Castellano, Polyhedron 17 (11–12) (1998) 2013.

[55] T. Mosmann, J. Immunol. Methods 65 (1–2) (1983) 55.

[56] U. Ziegler, P. Groscurth, Physiology 19 (3) (2004) 124.

[57] A. Levina, A. Mitra, P.A. Lay, Metallomics 1 (2009) 458.

[58] B. Peña, R. Barhoumi, R.C. Burghardt, C. Turro, K.R. Dunbar, J. Am. Chem. Soc. 136 (22) (2014) 7861.